IEEE Access
Multidisciplinary ⋮ Rapid Review ⋮ Open Access Journal

Received November 28, 2019, accepted December 5, 2019, date of publication December 10, 2019,
date of current version December 31, 2019.

Digital Object Identifier 10.1109/ACCESS.2019.2958678

Operation of Stand-Alone Microgrids Considering the Load Following of Biomass Power Plants and the Power Curtailment Control Optimization of Wind Turbines

ZHICHAO ZHOU[1,2], CHENGSHAN WANG[1], (Senior Member, IEEE), AND LEIJIAO GE[1], (Member, IEEE)

[1]Key Laboratory of Smart Grid of Ministry of Education, Tianjin University, Tianjin 300072, China
[2]CITIC Financial Leasing Company, Ltd., Beijing 100020, China

Corresponding author: Leijiao Ge (legendglj99@tju.edu.cn)

This work was supported by the National Natural Science Foundation of China under Grant 51807134.

ABSTRACT Various stand-alone hybrid power systems are widely used to fulfil the electric loads for remote, rural villages. Although there are many investigations based on various aspects of renewable hybrids energy microgrids, the discussions about the application of biomass combustion power plants are rare. Also, detailed investigations of the system steady and transient stability analysis, and the power curtailment control optimization of wind turbines in these stand-alone hybrid systems are seldom found. This paper focuses on wind/biomass/diesel/battery stand-alone microgrids and discusses the system operation, energy management and dispatch issues detailed. The renewable and controllable biomass power is localized to follow the load fluctuations over a long timescale to decrease the power production from diesel and the peak-load shifting demands of the battery banks. An optimization strategy of the wind power curtailment control is also proposed to effectively decrease the frequency and amplitude of the pitch actor and, to some extent, improve the power generation through the combination of the active turbine speed control and pitch regulation. Then a parallel double-mode optimal operation strategy with a ''fault detector'' is presented to realize economic optimization dispatch under the normal mode and emergency power control for large disturbance scenarios. Finally, case studies of a microgrid on a remote Canadian aboriginal community are conducted to demonstrate the performance of the proposed methods.

INDEX TERMS Stand-alone microgrid, biomass power plant, load follow, wind power curtailment control, energy management and dispatch, emergency power control.

I. INTRODUCTION

Remote, rural, stand-alone hybrid power systems are usually equipped with diesel engines (DEs) and battery banks, as well as wind turbine generators (WTG) and photovoltaic arrays (PV), depending on the locally available renewable energy resources [1]. There are many investigations based on various aspects of diesel-renewable hybrid stand-alone microgrids (SAMGs). The optimal sizing and the dynamic performance of an off-grid wind/diesel hybrid system have been analyzed by [2]. All the possible optimization solutions of stand-alone PV/wind/diesel/battery hybrid systems have been proposed in [3] with HOGA (Hybrid Optimization by Genetic Algorithms) software, and the results show that the utilization of suitable DEs can bring both economic and environmental benefits, when compared to the fully renewable energy systems. Also, studies on four different cases of a renewable based hybrid system have been carried out in [4] using the HOMER (Hybrid Optimization Model for Electric Renewables) software, and the analysis also reveal that the diesel-renewable mixed microgrid has the lowest net present cost (NPC) and a fairly small carbon footprint.

However, due to the intermittent nature of wind and solar energy resources and load demands, the controllable distributed generations (DGs) alone with some other technical approaches are quite necessary. So, DEs and/or battery banks are widely used to match the system instantaneous net load demands [1]–[4]. But in diesel-renewable hybrid SAMGs, the energy production from diesel is still high. Alternatively, in fully renewable-based systems, expensive energy storage

The associate editor coordinating the review of this manuscript and approving it for publication was Salvatore Favuzza.

battery banks with large capacities are needed. Also, various biodiesel fuels have been used in SAMGs [5], [6], biomass gasifier has been introduced in [7], and reverse osmosis desalination systems have been discussed in [8], [9]. Hydrogen energy storage and advanced rail energy storage system are also gained interests as in [9], [10]. From the load side, load forecasting has been suggested by [11], [12], demand response and adjustable power have been considered by [13].

Although various combinations of PV, WTG, biomass gasifier, biodiesel, battery and DE, together with load forecasting and demand response techniques, are proposed to address the electricity supply issues for remote areas, the discussions about the application of biomass combustion power plants are rare. In contrast to the intermittent wind and solar, biomass is a ubiquitous green renewable resource with good storability. Biomass combustion power technology is mature than biomass gasifier and biodiesel technologies, and gains widely applications in power generation industry. In the past, because of the high unit capacity, complex technology, and the professional operation and maintenance, this technology is not practically and economically affordable in SAMGs. But at present, with the growing progress in organic rankine cycle (ORC) technology, an increasing amount of ORC-based biomass power plants (BPGs) are being put into use [14], [15]. Compared to traditional steam turbine BPG, the main advantages of the ORC BPGs are the flexible unit capacity, high cycle efficiency, simple start-stop procedures, quiet operation, minimum maintenance requirements and good partial load performances [14], [15].

Optimum sizing design is an essential aspect for a hybrid energy system with minimal cost and maximal reliability, but not the all. Energy management and system stability operation are also very key factors. Various dispatch strategies in remote hybrid power systems have been modeled by [16], and the results illustrate one of two simple diesel dispatch strategies, either load following or full power for a minimum run time, can gain the cost-effective performances. The component layer and top layer controls have been proposed by [17], in which the power smoothing of battery is critical and the case studies based on a typical campus microgrid have been carried. Taking controllable loads, user's behavior and duty cycle of the appliances into account, an optimum load management strategy for wind/diesel/battery microgrids has been proposed by [18]. Hierarchical energy management systems (EMSs) have also been discussed by [19], [20], and the multiagent based EMSs have been introduced further in [12], [13].

Although previous studies have developed effective EMS strategies to keep the energy balance between the generation and the demand at hourly time intervals, they have not considered the actual power balancing in real time operation, and the system steady and transient stability analysis is seldom considered. This problem may be neglected for grid dependent microgrids [20]. But for SAMGs with little system inertia and great uncertainties in both generations and loads, the sufficient power reserve margin for the system safe and stable operation must be considered seriously, especially at the times when the systems suffer from big disturbances.

In addition, for WTG renewable based SAMGs, some of the wind energy is destined to be wasted as spilled energy because there is more excess renewable energy than the battery can hold and the SAMG can consume, especially when the wind is strong or/and the system is put into operation at the early lifecycle [16]. Thus, the wind power curtailment control (WPCC) will be a normal operation mode for WTG in SAMGs. There are two reasons. First, when taking the cost of fuel, fuel transportation in rugged terrains and the operation and maintenance costs into account, WTG is one of the most cost-effective and ecologically sound technologies compared to DE and BPG, so the high ratio penetration of wind power is very important for the economical operation of these hybrid power systems. Second, to build up all the DGs at one time to avoid a second construction when the load demands of the rugged terrain keep increasing in the future, and to generate more renewable energy under most possible conditions at middle and low wind speeds, the installation capacity of the WTG is often surplus to some extent.

For the variable-speed variable-pitch (VSVP) WTG, the power control, which mainly includes the rotor speed control (RSC) and pitch angle control (PAC), is very complicated [21]–[24]. The PAC has been widely used for VSVP WTGs under the WPCC situation. A hierarchical architecture with a supervisory control system controlling the active and reactive power of the whole wind farm and each particular turbine control system ensuring that the received power set points are reached through the PAC has been presented by [25]. The PAC using a generalized predictive control has been introduced to level the output power by [26], but this approach brings an unavoidable drop in the generation and is more useful for SAMGs. A robust PAC strategy which consists a nominal inverse-system controller and a robust compensator has also been proposed by [27]. Three turbine level curtailment strategies with four design objectives have been discussed by [28], and the results show that the strategy C, derates first only in torque at higher power points and later in both speed and torque, can meet all the design objectives.

In the previous literatures, fast and accurate power setpoint tracking is achieved through the PAC, but these methods also cause high pitch activity, fatigue loads and even drops in the output power. In fact, such setpoint tracking can also be achieved by the RSC. In [29], WTG is controlled in three operating modes (free running mode under medium wind condition, PAC mode under high wind condition and modified linear slope control mode under low wind condition) to follow operator's command with the consideration of generation margin assessment and spinning reserve support in SAMGs. However, very short term wind speed forecast is needed, and the changeovers of control modes have not been presented detailed.

In this paper, an optimal operation and control for biomass combustion power based SAMGs is proposed and the system

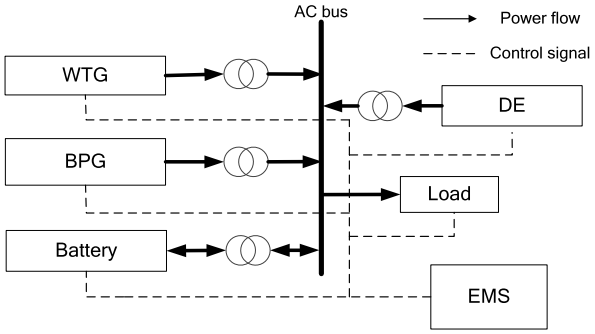

FIGURE 1. Structure of a wind/biomass/diesel/battery SAMG.

steady and transient stability analysis, together with the WPCC of WTGs, are presented. In Section II, the load following of renewable and controllable BPGs is introduced to decrease the power production from diesel and the peak-load shifting demands of the battery banks. Also, a WPCC strategy is addressed in Section III to effectively decrease the frequency and amplitude of the pitch actor and, to some extent, improve the power generation through a combination of active turbine speed control and pitch regulation. Furthermore, a novel parallel double-mode optimal operation strategy with a "fault detector" is then presented in Section IV to realize the economic optimization dispatch at the normal mode and the emergency power control under large disturbance scenarios. Finally, the case studies on a practical remote aboriginal community SAMG are conducted to demonstrate the performance of the proposed methods in Section V, followed by the conclusions.'

II. LOAD FOLLOWING CONTROL OF THE BPG

A. PROPOSED LOAD FOLLOWING CONTROL

The structure of a typical wind/biomass/diesel/battery SAMG is presented in Fig. 1. In this system, DEs are the most reliable DG, with good power dynamic response characteristics, thus very suitable for acting as the main power source. Wind power is renewable, ecological and the most cost-effective, but its output is intermittent and uncontrollable. Biomass power is both renewable and controllable, but its power dynamic response characteristics are poorer than that of DEs. Taking the cost of fuel, transportation and maintenance into account, the ranking of cost per kWh from low to high is wind, biomass and diesel. Therefore, the renewable and controllable biomass power is suitable for following the load fluctuations over a long timescale to decrease the power production from diesel and the peak-load shifting demands of the battery banks, thus achieving an effective cooperation with wind power. The load following strategy based on biomass combustion power plant is described as follows:

1) DEs still run as the main power source in the SAMG to match the instantaneous net load, but the operating point is set at a relatively low setpoint $P_{\mathrm{D\_base}}$ to reserve a larger power consumption space for the wind and biomass power, and also to hold enough spinning reserve for the system operation.

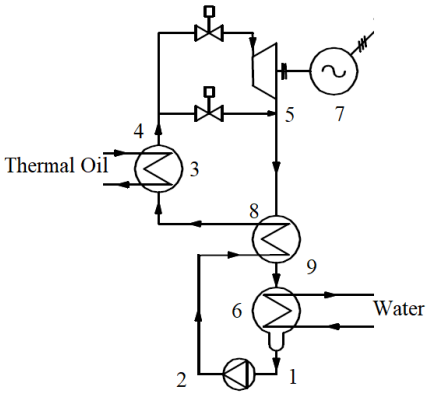

FIGURE 2. Components schematic of ORC.

2) BPGs serve as the auxiliary power supply to follow the net load over a long timescale to decrease the diesel power production. Because of the limitations of the minimum run time and minimum start-up time, and benefitting from the low minimum allowed operation power of the ORC turbogenerator, the BPG runs at all times to avoid excessively frequent start/stop.
3) WTGs are used to generate as much energy as possible at the maximum power point tracking (MPPT) mode under the high net load conditions, or work at WPCC mode because of the constraints of the system's safe and stable operation. High wind power penetration and low wind power curtailment should be considered at the same time.
4) Battery energy storage system (BESS) is first set to give emergency power control in case of large disturbances to help the system maintain stability together with DEs. Then, it provides peak load shifting to improve the matching between the wind power and load demands. Through this method, the BESS capacity size can be optimized, and the charge/discharge times can also be remarkably decreased.

B. BPG BASED ON ORC

ORC based BPG is considered in this paper due to its flexible unit capacity and high automation. The ORC unit is based on a closed Rankin cycle performed by adopting a suitable organic fluid as the working fluid [14], [15]. Fig. 2 shows the relevant components of an ORC unit [15].

There are three fluids in Fig. 2: water, thermal oil and organic fluid. The thermal oil (approximately 310°C) is heated by the biomass fired combustion system to preheat (2→8) and vaporize (8→3) the organic working fluid in the evaporator. Part of the organic fluid vapor powers the turbine to drive the electric generator (4→5→7). The exhaust vapor, together with the directly extracted vapor, flows through the regenerator (5→9) to heat the organic fluid. In the water-cooled condenser, the vapor is finally condensed (9→6→1) and then pumped to the regenerator (1→2). Through this closed operation circuit, the following advantages can be obtained: high cycle efficiency (especially in combined heat and power plants),

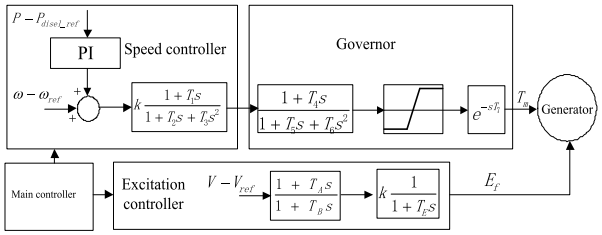

FIGURE 3. Control diagram of the BPG.

long operational life, good partial load performance, simple operation procedures and minimum maintenance requirements. Compared to traditional steam turbines, no particular qualification is required for the personnel operating of ORC plants, which is very important for customers without a specific electricity background in remote rural communities.

The dynamic model of a BPG is shown in Fig. 3 in [30]. The terminal voltage is regulated by the excitation system, and the speed of the synchronous generator is controlled by the speed controller. The main controller compares the bus voltage and the frequency with the reference values and then achieves synchronization switching.

III. PROPOSED N-WPCC STRATEGY

A. ORDINARY POWER CONTROL OF VSVP WTG

In ordinary power control (OPC), to obtain the possible maximum output power over a wide range of wind conditions, the WTG should always operate in the MPPT mode, which is also called the maximum C_p mode. However, for safety and economic reasons, there are limits on both the generator speed and the output power, thus the power control of the VSVP WTG is divided into four operation modes, as shown in Fig. 4. In the first mode at low wind speeds just above cut-in speed v_1, the turbine is operated at a constant generator speed ω_{min} because of its minimum limitation. In the second mode at moderate wind speeds ($[v_2, v_5]$), the generator speed begins to vary with the wind speed to obtain the maximum C_p, to harvest maximum power from the wind. This mode is the normal operation region, but when the generator speed is increased to its maximum value ω_n as the wind speed reaches v_5, the control switches into the third mode. In the region at higher wind speeds ($[v_5, v_6]$), the turbine is again operated under constant speed ω_n, and C_p begins to decrease slowly. In the first three modes ($[v_1, v_6]$), the wind turbine speed is regulated according to the wind speed, and the blade pitch control keeps stand-by. In the fourth mode above the rated wind speed ($[v_6, v_7]$), the output power is kept constant at the rated power by regulating the blade pitch system. For very high wind speeds above the cut-out speed v_7, the turbine will be shut down for safety. In Fig. 4, the operating point D represents the fourth mode.

From Fig. 4, the power and speed relationship can be expressed as

$$\begin{cases} \omega = \omega_{min} & P_e < P_B \\ \omega = \omega_{opt} = f(P_e) & P_B \le P_e < P_C \\ \omega = \omega_n & P_e \ge P_C \end{cases} \quad (1)$$

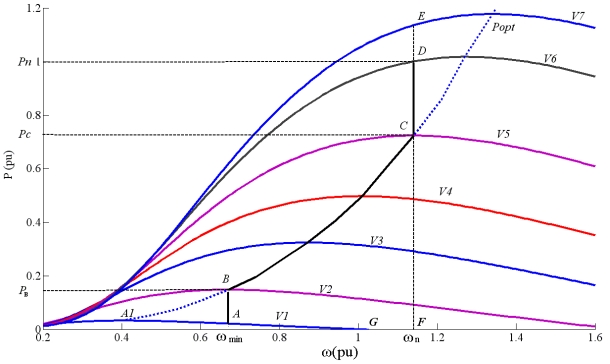

FIGURE 4. Power speed relationships at different wind speeds.

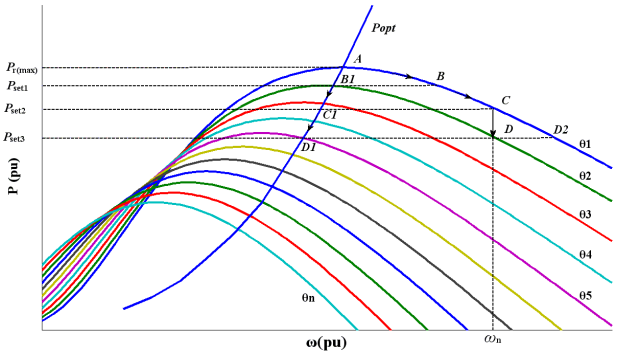

FIGURE 5. Schematic diagram of WPCC at a moderate wind speed.

B. OPTIMAL WPCC STRATEGY

The objective of the WPCC is to decrease the power coefficient C_{Pmax} to some other value C_{Pset}, thus decreasing the captured wind power to the set point P_{set}. The regulation of C_P can be achieved by control of both the blade pitch angle θ and the tip speed ratio λ [22], [23]. Due to the maximum speed limitation, PAC is the only method that can realize WPCC at higher wind speeds (above v_5 in Fig. 4). However, RSC can also work in the WPCC mode at medium and low wind speeds ($[v_1, v_5]$). To discuss this scenario in detail here in Fig. 5, which presents a set of power speed curves of a VSVP WTG at a given moderate wind speed with different pitch angles (from $\theta_1 = 0°$ to θ_n, increasing in intervals of 1.5°). Operation point A indicates the maximum available output power $P_{r(max)}$. In T-WPCC, the output power is regulated by θ, and the rotor speed is decided passively by the P_{opt} curve. Therefore, B_1, C_1 and D_1 are the operation points corresponding to P_{set1}, P_{set2} and P_{set3}, respectively. At all the wind speeds, the T-WPCC track can be illustrated as the curve DCBA in Fig. 4, which is just opposite to that of the OPC.

As seen in Fig. 5, the WPCC can also be achieved by actively regulating the rotor speed. Operation point B also indicates the curtailed output power P_{set1}, with a proper higher rotor speed, without θ regulation. Point C represents the possible curtailment space just through RSC. When the power command is below P_{set2}, e.g., P_{set3}, the WPCC should then be finished through both RSC and PAC together.

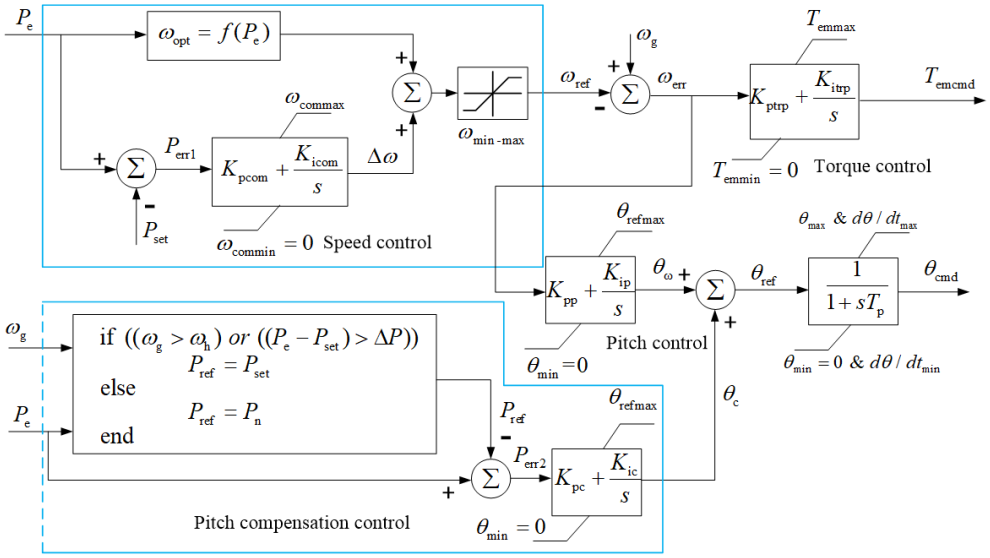

FIGURE 6. N-WPCC model block diagram.

Both D and D_1 are stable operation points corresponding to P_{set3}, but the former has a smaller θ and a higher speed. This means that N-WPCC can translate part or all of the surplus wind energy into the turbine rotational energy by actively increasing the rotor speed, and the stored energy can be converted back into power when the curtailment conditions are alleviated (i.e., a drop in the wind speeds or an increase in the power command). In Fig. 4, the line DC and the region ABCFGA represent the operational space of N-WPCC at all wind speeds.

Compared to T-WPCC, N-WPCC can effectively decrease the frequency and amplitude of the pitch regulation, and it can also improve the power production to some extent. These are beneficial for the economical and reliable operation of WTGs in WPCC.

C. N-WPCC CONTROLLER DESIGN

The assumed design objectives of N-WPCC are giving priority to RSC over PAC, not affecting the normal performances of the MPPT and producing smooth switchovers between the WPCC and normal MPPT modes. The proposed N-WPCC controller consists of four subsystems: the RSC, the torque control, the PAC and the pitch angle compensation control, as shown in Fig. 6.

In the N-WPCC, there are two major modifications compared with the T-WPCC. First is the RSC, which is designed as

$$\begin{cases} \omega_{ref} = \omega_{opt} = f(P_e) & P_e \le P_{set} \\ \omega_{ref} = \min(\omega_{opt} + \Delta\omega, \omega_n) & P_{set} < P_e \end{cases} \tag{2}$$

where ω_{ref} is the rotor speed reference, which is equal to ω_{opt} in the MPPT or the sum of ω_{opt} and an additional $\Delta\omega$ in the WPCC.

Second is the soft switching of P_{ref} in the pitch angle compensation control, which is performed by the following:

$$\begin{aligned} &\text{if } ((\omega_g > \omega_h) \text{ or } ((P_e - P_{set}) > \Delta P)) \\ &\quad P_{ref} = P_{set}; \\ &\text{else} \\ &\quad P_{ref} = P_n; \\ &\text{end} \end{aligned} \tag{3}$$

where ω_g is the real-time rotor speed, ω_h is a high value slightly below ω_n, and ΔP is the power control error limitation. This soft switching rule ensures that only when the turbine speed reaches close to the rated speed can the PAC be activated to vary the pitch angle. Otherwise, the RSC is the only activated way of realizing the WPCC. When C_p decreases very slowly with an increase in ω_w around the top of the power speed curve, e.g., near point C in Fig. 3, the effect of the RSC is limited, so the criterion ΔP is used to quickly activate PAC. In addition, a hysteresis control is set to avoid frequent switchovers.

In Fig. 6, the speed variable $\Delta\omega$ is the output of the proportion integral (PI) controller, where the power error $P_{err1}(P_e\text{-}P_{set})$ is used as the input, so the speed reference ω_{ref} increases under the maximum limitation when $P_{set} < P_e$. The pitch compensation control is same as in the T-WPCC, except that the power reference P_{ref} is given by the soft switching function.

When P_{set} increases or the actual wind speed drops, and thus the curtailment condition is relieved, P_{err1} will change from positive to negative, and $\Delta\omega$ will begin to decrease until reaching zero. For the same reason, θ_c will also decrease. But compared with large turbines with large inertia time constants, the dynamics of the PAC are moderately fast, so the PAC responds quickly; the rotor speed begins to decrease only when θ reaches zero. Obviously the operation characteristics

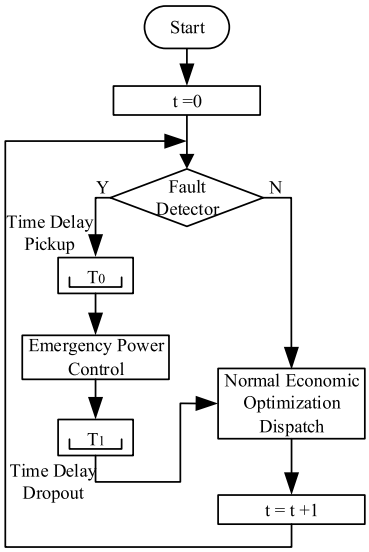

FIGURE 7. Schematic diagram of the double-mode optimal operation.

at this moment are opposite to N-WPCC, which are indicated as the solid line DCBA in Fig. 4. This is to say, the reverse control of N-WPCC is achieved first by the RSC and then by the PAC as necessary, so the control effect of N-WPCC is reversible.

In addition, N-WPCC has good versatility and a practical engineering value because it only requires the output power and rotor speed for its control inputs without requiring the actual wind speed.

IV. PARALLEL DOUBLE-MODE OPTIMAL OPERATION

A. SCHEMATIC DESCRIPTION

According to the operation characteristics of DGs in the wind/biomass/diesel/battery SAMG, a novel parallel double-mode coordinated operation management is proposed considering economic, environmental and safety aspects. In the economic optimization dispatch at the normal mode, DEs and BPGs are used to follow the load fluctuations over the instantaneous and long timescale respectively, and BESS is mainly in standby state. In the emergency power control for large disturbance scenarios, DEs, together with BESS, are then used to maintain the system stable through the coordinating with different action times. Fig. 7 shows the schematic diagram of the double-mode optimal operation.

A ''fault detector'' based on the real output power of the running DEs is set to detect whether the SAMG suffers severe fluctuations. As discussed in Section II, the DEs should run around the settable power under normal economic operation. When severe fluctuations occur, perhaps from intermittent resources and loads, the DEs, as the main power source in the SAMG, will immediately absorb the instantaneous unbalance power. This action may make the DEs work under light or heavy load conditions. In this scenario, the ''fault detector'' is trigged, the system status flag is transferred to ''1'', and this scenario is identified as the fault status ''C_1''. When the fault status continues for a short time (as shown in Fig. 7, the settable time delay pickup T_0), the emergency power control is activated. BESS is used to provide a larger charge/discharge power quickly in order to help the system maintain stability together with the DEs, which is identified as the transition status ''C_2''. The emergency power control mode will continue until the settable time dropout T_1 ends. After that, SAMG will return to normal economic optimization dispatch, and the new steady state is identified as ''C_3''.

In this strategy, the ''fault detector'' is very sensitive, but a time delay T_0(T_0 = 2 s in the following case) is required to confirm the ''fault'', thus ensuring that the detector is reliable. The settable time dropout T_1, which equals 10 s in this paper, is a longer time than T_0 to wait for the fault clearance; however, this delay limits the state transition time to a reasonable period, which controls the BESS capacity at an economic size.

B. OBJECTIVE FUNCTIONS AND CONSTRAINTS

The multi-objective optimization model aims to minimize the NPC and the pollutant emission level in the 20 years full life cycle. That is,

$$Min\, f_i(X) \quad \mathrm{i} = 1, 2 \tag{4}$$

Here, f_1(X) is the NPC includes the equipment replacement, fuel, operation and maintenance, and the residual value. And f_2(X) is the pollutant emission amount from diesel.

For power reliability, the loss of power supply probability (LPSP) is used for the design of SAMG, which can be written as follows:

$$LPSP = \frac{E_{CS}}{E_{tot}} \leq 0.01 \tag{5}$$

where E_{CS} and E_{tot} denote the shortage energy and the total electricity demand respectively. Here, the maximum allowable LPSP is 0.01.

Spinning reserve support at both the normal operation mode and the emergency power control mode is also considered in this paper as follows:

$$P_{res\_nor}(t) = r_{ld}P_L(t) + r_{pl}P_{L\_p} + r_wP_W(t) \tag{6}$$

$$P_{res\_em}(t) = \max\{0.1 \times P_{L\_p}, \max(P_D(t), P_W(t), P_B(t), P_E(t))\} \tag{7}$$

Here, P_{res_nor} and P_{res_em} denote respectively the power spinning reserve for the normal mode and the emergency mode, $P_L(t)$, $P_W(t)$, $P_B(t)$ and $P_E(t)$ are load, WTG output, BPG output and BESS output at t, P_{L_p} is the annually peak load, r_{ld}, r_{pl} and r_w are the corresponding capacity ratio factor.

The rest common constraints, such as power balancing, operation bounds for BPGs and DEs, charging/discharging and SOC limitations of BESS are similar to those presented in [3], [9], [13], so are not written detailed here.

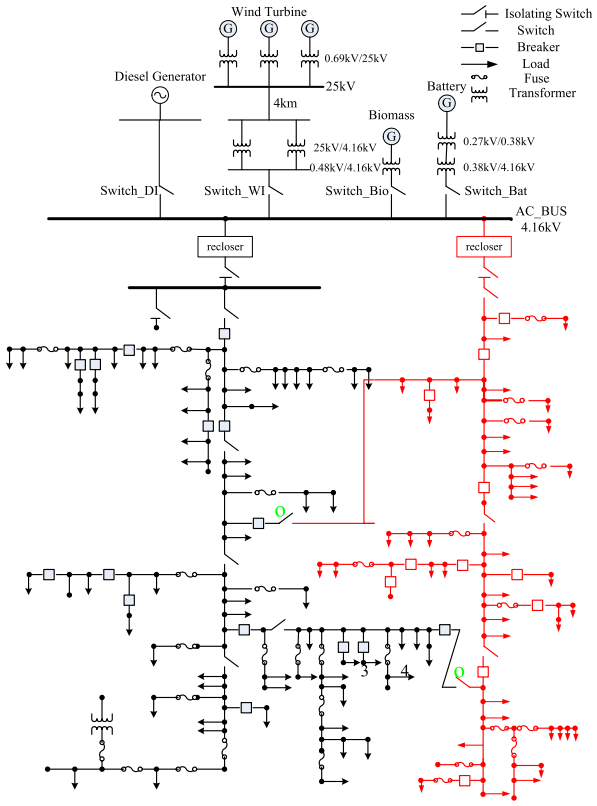

FIGURE 8. System setup of a typical wind/biomass/diesel/battery SAMG.

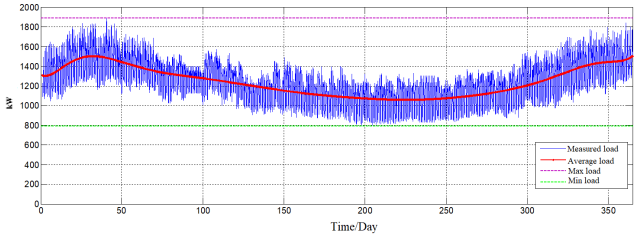

FIGURE 9. Actual annual load analysis diagram.

V. CASE STUDIES

A. CASE DESCRIPTION

A typical wind/biomass/diesel/battery SAMG in a remote aboriginal community (55°16′ N, 77°45′ W) in Canada is taken as a case to study the correctness and validity of the proposed methods in this paper. This microgrid, which consists of 3∗1.5 MW WTGs, 1*1.0 MW BPG, 3*1.1 MW DEs (which are the power sources of the existing system), and 2 MW*1 h BESS, as shown in Fig. 8, is proposed to provide the electricity for the community for the next 20 years. The annual average wind speed at a hub height of 65 m is 7.45 m/s, and the distribution probability of winds less than the speed corresponding to 0.7 p.u. of the WTG rated power (9 m/s in this case) is 72.4%.

Fig. 9 shows the actual hourly electricity demand in a whole year. The red solid curve represents the daily average load, and the blue solid curves denote the real-time load. In this paper, the following load demand forecasts are derived from the historic datum, with an annually increasing of 3%. And the wind datum over the 20 years are deduced from the historical wind speed in typical years with a time interval of 10 minutes. A 10% random fluctuation is added to better simulate the uncertainty of wind.

TABLE 1. The main parameters used in the simulation.

Parameters	Value
WTG	
WTG rotor radius	38.5m
Air density	1.225 kg/m^3
Cut-in wind speed	3m/s
Cut-out wind speed	25m/s
Nominal wind speed	11.1m/s
Rated turbine rotational speed	1.7829rad/s
Rated rotational speed	1750rpm
Optimal tip speed	7.8
Maximum *Cp*	0.50
Stator resistance/inductance	1.10mΩ/0.17mH
Rotor resistance/inductance	0.86mΩ/0.13mH
Exciting inductance	1.83mH
Moment of inertia	2.95×10^{6}kg.m^2
DE	
Minimum allowed power	0.3p.u
Maximum allowed power	1.5p.u
P_{D_base}	0.5p.u
Intercept of the consumption curve	0.016 L/h
Slope of the consumption curve	0.26 L/(kW • h)
Fuel price including transport	1.7$/L
BPG	
Minimum operation point	0.2p.u
Minimum running time	4h
Minimum start-up time	6h
Power dynamic response character	0.1p.u/10min
Nominal fuel consumption	2.44t/MW/h
Biomass price including transport	178$/t
BESS	
SOC_{min} for emergency	0.1
SOC_{max} for emergency	0.9
SOC_{down} for normal mode	0.3
SOC_{up} for normal mode	0.85
Low charge/discharge rate	0.2
High charge/discharge rate	0.6
Spinning reserve	
r_{ld}	0.1
r_{pl}	0
r_w	max(0, P_{set}/ P_n - 0.75)

In the following studies, the load following control of the BPG and the energy optimal allocation of DGs in the normal mode are carried out under the quasi-steady state simulations, with time intervals of 1 hour and 10 minutes respectively. The performances of the N-WPCC and the emergency power control in large disturbances are studied on the electromechanical transient simulation models in MATLAB/Simulink, and the simulation time step is 50us.

The main parameters related to the simulation are tabulated in Table 1.

B. LOAD FOLLOWING OF THE BPG

Three different load following methods of the BPG have been run in Fig. 10 to discuss their effectiveness. In the three cases, the BPG output power is respectively set at (1) constant but

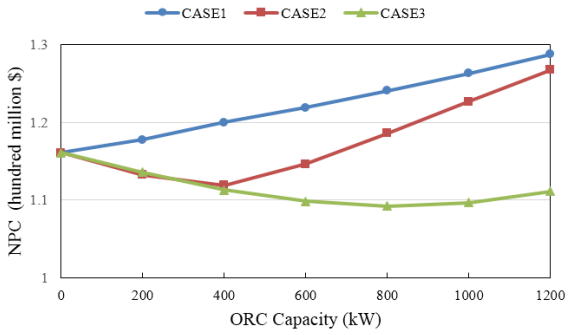

FIGURE 10. Economical sensitivity analysis of the BPG capacity with different dispatch strategies.

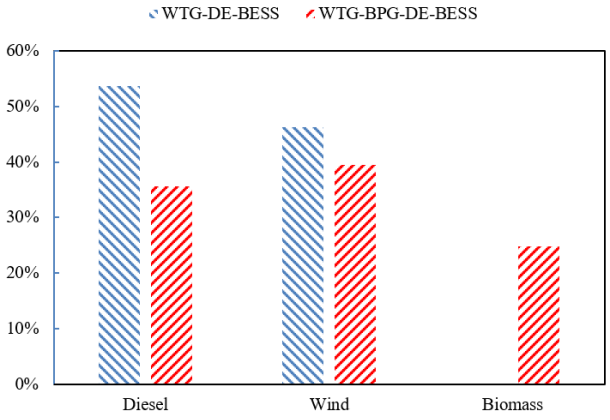

FIGURE 11. Analysis of the DGs output power ratio.

with an annual growth rate of 3%, the same as the annual growth rate of the load, (2) a 30% ratio of the real time load, and (3) a 30% ratio of the real time net load. However, as mentioned before, to avoid excessive start/stop, the BPG will run at the minimum permissible operation point even if there is surplus wind at that time.

Fig. 10 shows that the NPC almost appears to have linear growth with an increase in the ORC capacity in case 1, in which the constant operation point ensures the BPG output but also greatly squeezes the consumption space of the renewable wind. In case 2 and case 3, when the BPG capacity is relatively small compared to the entire SAMG, for example, less than 400 kW, the BPG has little influence on WTGs and DEs, so the NPC decreases. As the BPG capacity continues increasing, only case 3 can show better economics because the BPG output is determined by both the load and the wind, so the efficient combined power generation of the WTG and BPG is achieved. From Fig. 10, the turning point is approximately 1 MW, after which NPC begins to grow slightly.

Fig. 11 shows the output power of individual DGs in the WTG/BPG/DE/BESS SAMG compared with the WTG/DE/BESS solution. It shows that the diesel gives much less output power, from 53.2% to 35.0%, and the WTGs also clearly gives less power, from 46.8% to 39.2%, BPG contributes 25.8% of the energy. These results mean less cost for the diesel fuel and less pollutant emissions.

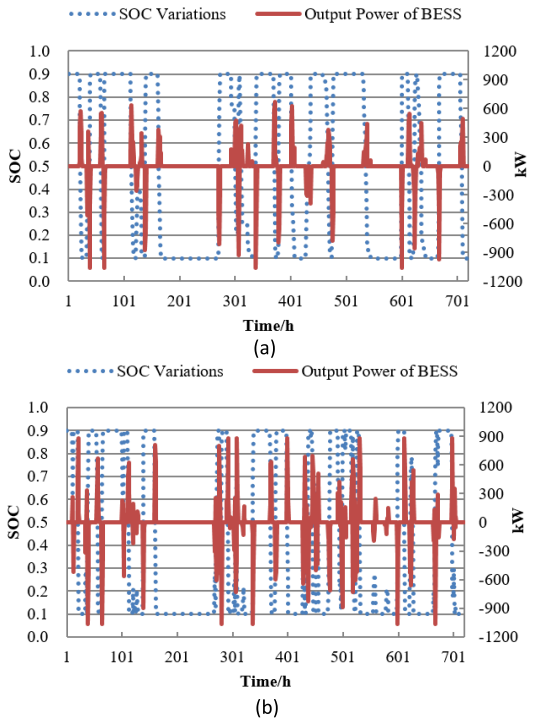

FIGURE 12. Typical operation situations of the BESS during a week.

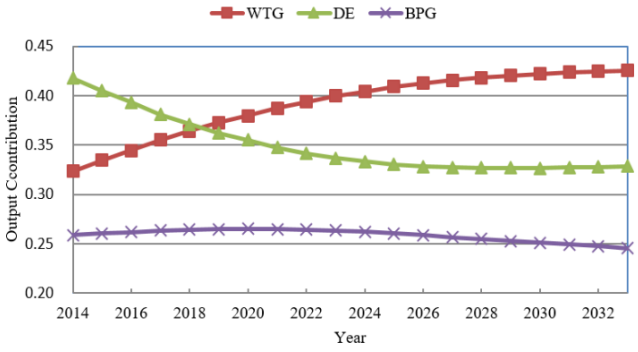

FIGURE 13. Yearly output contribution of DGs in 20 Years.

The typical operation situations of the BESS during an entire week are depicted in Fig. 12. With the load following the BPG, less SOC variation [blue dotted lines] and less frequent charge/discharge changeovers [red solid lines] are needed in Fig. 11(a) compared with those of the case without BPG in Fig. 11(b). Simulation studies show that the total energy transferred by BESS in this SAMG is 2.9 GWh, whereas the energy is 6.9 GWh without BPG. Therefore, the load following of the BPG can greatly optimize the capacity size and operational conditions of the BESS.

C. N-WPCC OF WTGs

Fig. 13 gives the annual output power contribution curves of the different DGs over the whole 20-year lifetime. With an annual increase in the electricity demand, the energy contribution of the WTGs increases gradually, and the corresponding curtailed power ratio drops gradually from 67.9%

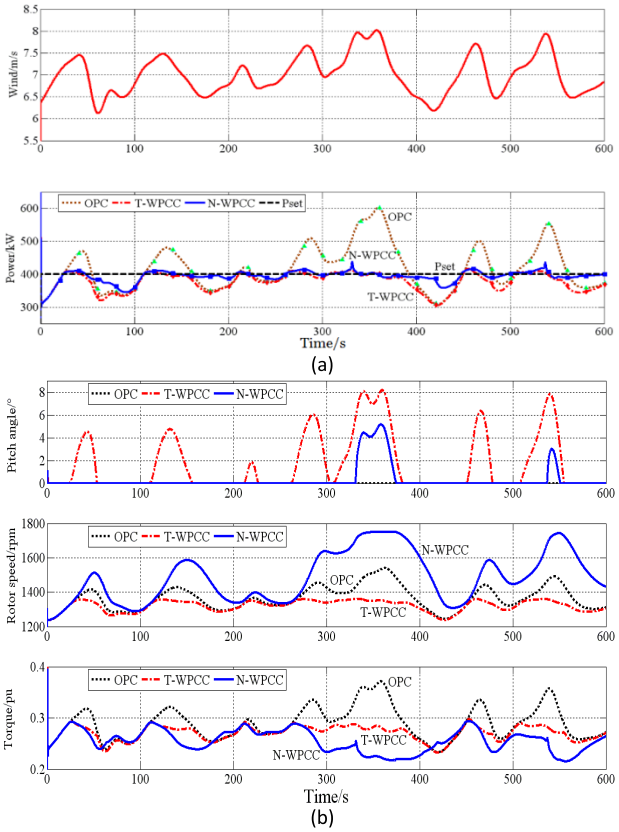

FIGURE 14. Dynamic responses of the three power control strategies at random wind speeds (a) Wind speed and output power. (b) Pitch angle, rotor speed and electromagnetic torque.

in the first year to 28.7% in the 20th year. Although the curtailed wind power ratio is rather high, the SAMG achieves a comprehensive optimal operation because the wind power is the most cost-effective and ecologically sound energy in this SAMG. This result demonstrates that a high wind power penetration means good economic and environmental benefits, but it also means a high wind power curtailment.

To better understand the effectiveness of N-WPCC, Fig. 14 is presented, in which the wind is random for 600 s. It shows that the N-WPCC has better performances than the T-WPCC: (1) the pitch angle regulation times drop from 7 to 2, (2) the pitch angle regulation amplitude declines obviously, varying from approximately 3° to 5°, and (3) the P_e distribution curve is more concentrated near P_{set} and is higher, to some extent, at several moments (the calculated results show that N-WPCC improves the output power by 1.6% compared with the T-WPCC under this scenario). Additionally, from the simulation results, we can see that the WPCC can make the WTG act as a controllable power source in some special conditions. It is helpful for the load following in SAMG applications.

D. OPTIMAL ALLOCATION AND ECONOMIC ANALYSIS OF THE MULTIPLE DGS

Fig. 15 shows a snapshot of the DGs performance in the steady normal mode. 3 typical scenarios are selected to discuss the optimal allocation of the different DGs.

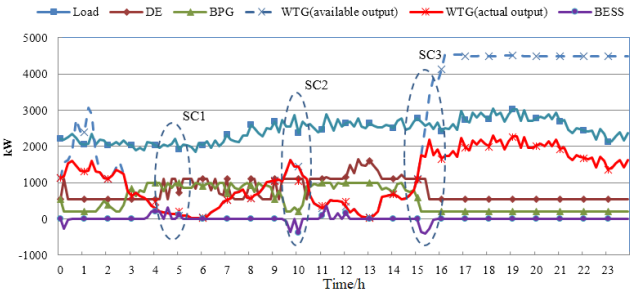

FIGURE 15. Typical daily operation power curves of DGs.

SC 1: When the wind becomes increasingly insufficient, first the BPG output power is gradually improved until it reaches its rated power; then, the BESS begins to discharge under the limitation of 400 kW, even starting a new DE when the SOC of the BESS decreases to SOC_{down}.

SC 2: The output power of BPG decreases while the wind power increases with the growth of the wind. When the BPG reaches 200 kW, it keeps stable, and the BESS begins to charge with the limitation of 400 kW. One DE is cut off when the SOC of BESS increases to SOC_{up}.

SC 3: The wind becomes surplus and the WTGs are running at WPCC mode. The BPG runs at 200 kW, the BESS transfers to standby under the limitation of SOC_{up}, and only one DE is needed to run.

Fig. 15 shows that WTGs run under the MPPT control to output the maximum power at low wind speeds, and run under the WPCC to limit the impact on the system stability at high wind speeds. The BPG output power is higher at the higher net loads conditions to decrease the power from diesel. At the lower net loads, the BPG runs at its minimum allowed operation power to avoid the frequently start/stop times, though, it squeezes the consumption space of wind power further. DEs run at all times with different unit commitments according to the real time net loads and spinning reserve requirements. BESS works as standby at most times except for some scenarios with big fluctuations of the net load.

E. EMERGENCY POWER CONTROLLER FOR LARGE DISTURBANCES

Fig. 16 shows the simulation results when a WTG is suddenly trigged at a relatively high wind speed (keeps constant at 9.5 m/s during the short 25 s fault period). It shows that the instantaneous large power vacancy is taken over first by the running DE, causing the DE overload temporarily, then the "fault detector" is trigged, the system is transferred into the fault status. During a next short time ($T_0 = 2$ s), when the fault status is still on, the BESS is trigged to discharge at a high discharge rate to send the DE back to its normal state, and the system is transferred into the transition status. During another short time ($T_1 = 10$ s), when the large disturbances don't happen again, the emergency power control mode ends, and the BESS returns to the charge state at a low rate. Therefore, under the large disturbance conditions,

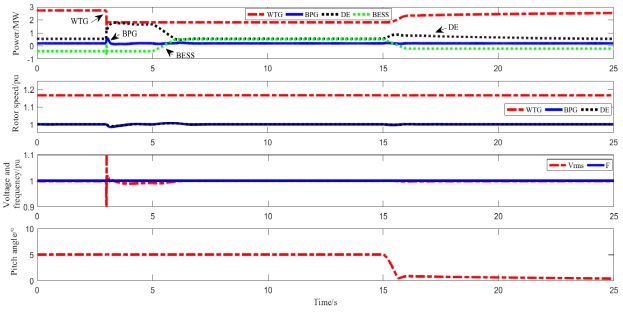

FIGURE 16. Transient stability simulation when a WTG is suddenly shutdown.

the BESS is set to provide the emergency power control with only 10 s. After the fault clearance, the BESS returns to the normal charge/discharge state right now to make the SOC recover to its normal scope. Through this method, the BESS can be always available for the next large disturbance, and its capacity is also optimized at an economic size.

Fig. 16 also presents the operation characteristics of the three WTGs. Before and during the failure, the WTGs are under WPCC conditions. After the clearance of the failure, the remaining two WTGs begin to run at the MPPT mode. The output power is 0.61 p.u. before 15 s and then reaches 0.84 p.u. The pitch angle decreases from approximately 5° to 0 correspondingly. However, the rotor speed is kept constant at the nominal value at all times because of the aforementioned N-WPCC control strategy.

VI. CONCLUSION

In this study, a hybrid biomass combustion power plant based wind/biomass/diesel/battery SAMG is suggested and the system operation with the considerations of the system steady and transient stability analysis and the WPCC strategy of WTGs is investigated. Through following the net load between the load and the wind power, the BPG can achieve an efficient combined power generation with WTGs, thus greatly decrease the power production from diesel and release the regulation stress of BESS for peak load shifting. And for WTGs in WPCC conditions, the active turbine speed control is proposed to optimize the operation and to some extent make the turbines act as a controllable power source, together with the pitch regulation at necessary. Also, a new parallel double-mode operation approach with a ''fault detector'' has been presented to productively bring economic, environmental and reliable benefits for the system energy management and dispatch, also to effectively limit the medium transition status during large disturbances. The proposed methods are finally tested and verified by case studies of a remote Canadian aboriginal community SAMG.

With the expected continuing development in biomass combustion power technology, as well as advances in providing local employments and improving the income and educational level of local residents, BPG will become a more promising solution for SAMG in remote locations, and the energy cascade utilization of biomass, such as combined heat and power technology, will likely gain more concerns. Also, alone with the increasing capacity of the SAMG, more and more MW level WTGs will be increasingly used, the discussion of WPCC for WTGs will be more interesting. And the improving reliability of power supply will also make the consideration of the system stability analysis necessary.

REFERENCES

[1] R. Luna-Rubio, M. Trejo-Perea, D. Vargas-Vázquez, and G. J. Ríos-Moreno, ''Optimal sizing of renewable hybrids energy systems: A review of methodologies,'' *Sol. Energy*, vol. 86, no. 4, pp. 1077–1088, Apr. 2014.

[2] T. K. Saha and D. Kastha, ''Design optimization and dynamic performance analysis of a stand-alone hybrid wind–diesel electrical power generation system,'' *IEEE Trans. Energy Convers.*, vol. 25, no. 4, pp. 1209–1217, Dec. 2010.

[3] R. Dufo-López, J. L. Bernal-Agustín, M. Y. José, A. D.-N. José, J. R.-R. Ignacio, L. Juan, and A. Ismael, ''Multi-objective optimization minimizing cost and life cycle emissions of stand-alone PV-wind-diesel systems with batteries storage,'' *Appl. Energy*, vol. 88, no. 11, pp. 4033–4041, 2011.

[4] O. Hafez and K. Bhattacharya, ''Optimal planning and design of a renewable energy based supply system for microgrids,'' *Renew. Energy*, vol. 45, pp. 7–15, Sep. 2012.

[5] A. Maleki, A. Hajinezhad, and M. A. Rosen, ''Modeling and optimal design of an off-grid hybrid system for electricity generation using various biodiesel fuels: A case study for Davarzan, Iran,'' *Biofuels*, vol. 7, no. 6, pp. 699–712, 2016.

[6] D. Guangqian, K. Bekhrad, P. Azarikhah, and A. Maleki, ''A hybrid algorithm based optimization on modeling of grid independent biodiesel-based hybrid solar/wind systems,'' *Renew. Energy*, vol. 122, pp. 551–560, Jul. 2018.

[7] S. Ashok and P. Balamurugan, ''Biomass gasifier based hybrid energy system for rural areas,'' in *Proc. IEEE Canada Elect. Power Conf.*, Oct. 2007, pp. 371–375.

[8] G. Zhang, B. Wu, A. Maleki, and W. Zhang, ''Simulated annealing-chaotic search algorithm based optimization of reverse osmosis hybrid desalination system driven by wind and solar energies,'' *Solar Energy*, vol. 173, pp. 964–975, Oct. 2018.

[9] A. Maleki, ''Design and optimization of autonomous solar-wind-reverse osmosis desalination systems coupling battery and hydrogen energy storage by an improved bee algorithm,'' *Desalination*, vol. 435, pp. 221–234, Jun. 2018.

[10] M. Moazzami, J. Moradi, H. Shahinzadeh, G. B. Gharehpetian, and H. Mogoei, ''Optimal economic operation of microgrids integrating wind farms and advanced rail energy storage system,'' *Int. J. Renew. Energy Res.*, vol. 8, no. 2, pp. 1155–1164, 2018.

[11] W. P. Zhang, A. Maleki, and M. A. Rosen, ''A heuristic-based approach for optimizing a small independent solar and wind hybrid power scheme incorporating load forecasting,'' *J. Cleaner Prod.*, vol. 241, pp. 1–18, Aug. 2019.

[12] C. X. Dou, G. Xiao, and Y. Dong, ''Multi-agent system based energy management strategies for microgrid by using renewable energy source and load forecasting,'' *Electr. Power Compon. Syst.*, vol. 44, no. 18, pp. 2059–2072, 2016.

[13] V. Bui, A. Hussain, and H.-M. Kim, ''A multiagent-based hierarchical energy management strategy for multi-microgrids considering adjustable power and demand response,'' *IEEE Trans. Smart Grid*, vol. 9, no. 2, pp. 1323–1333, Mar. 2018.

[14] *Generation of Clean and Renewable Electricity Using Organic Rankine Cycle (ORC) Technology*, PW Power Syst., Glastonbury, CT, USA, 2012.

[15] A. Duvia, A. Guercio, and C. Rossi, ''Technical and economic aspects of Biomass fulled CHP plants based on ORC turbogenerators feeding existing district heating networks,'' in *Proc. 17th Eur. Biomass Conf.*, Hamburg, Germany, 2009.

[16] B. C. Dennis and W. C. Byron, ''Optimal dispatch strategy in remote hybrid power systems,'' *Sol. Energy*, vol. 58, nos. 4–6, pp. 165–179, 1996.

[17] D. H. Zhu, R. Yang, and G. Hug-Glanzmann, ''Managing microgrids with intermittent resources: A two-layer multi-step optimal control approach,'' in *Proc. North Amer. Power Symp.*, 2010, pp. 1–8.

[18] J. M. Lujano-Rojas, C. Monteiro, R. Dufo-López, and J. L. Bernal-Agustin, "Optimum load management strategy for wind/diesel/battery hybrid power systems," *Renew. Energy*, vol. 44, pp. 288–295, 2012.
[19] Q. Y. Jiang, M. D. Xue, and G. C. Geng, "Energy management of microgrid in grid-connected and stand-alone modes," *IEEE Trans. Power Syst.*, vol. 28, no. 3, pp. 3380–3389, Aug. 2013.
[20] M. Mahmoodi, P. Shamsi, and B. Fahimi, "Economic dispatch of a hybrid microgrid with distributed energy storage," *IEEE Trans. Smart Grid*, vol. 6, no. 6, pp. 2607–2614, Nov. 2015.
[21] W. Leithead and S. Dominguez, "Active regulation of multi-MW wind turbines: An overview," *Power Syst. Technol.*, vol. 31, no. 20, pp. 24–34, 2007.
[22] W. M. Nicholas, J. S.-G. Juan, W. P. William, and W. D. Robert, "Dynamic modeling of GE 1.5 and 3.6 MW wind turbine generators for stability simulation," *GE Power Syst. Energy Consulting*, pp. 1977–1983, Jul. 2003.
[23] W. M. Nicholas, J. S.-G. Juan, and W. P. William, "Dynamic modeling of GE 1.5 and 3.6 MW wind turbine-generators," GE Power Syst. Energy Consulting, GE Company, Boston, MA, USA, Tech. Rep., Oct. 2003.
[24] A. Miller, E. Muljadi, and D. S. Zinger, "A variable speed wind turbine power control," *IEEE Trans. Energy Convers.*, vol. 12, no. 2, pp. 181–186, Jun. 1997.
[25] L.-R. Chang-Chien and Y. C. Yin, "Strategies for operating wind power in a similar manner of conventional power plant," *IEEE Trans. Energy Convers.*, vol. 24, no. 4, pp. 926–934, Dec. 2009.
[26] J. L. Rodriguez-Amenedo, S. Arnalte, and J. C. Burgos, "Automatic generation control of a wind farm with variable speed wind turbines," *IEEE Trans. Energy Convers.*, vol. 17, no. 2, pp. 279–284, Jun. 2002.
[27] A. S. Deshpande and R. R. Peters, "Wind turbine controller design considerations for improved wind farm level curtailment tracking," in *Proc. IEEE Power Energy Soc. Gen. Meeting*, Jul. 2012, pp. 1–6.
[28] T. Senjyu, R. Sakamoto, N. Urasaki, T. Funabashi, H. Fujita, and H. Sekine, "Output power leveling of wind turbine Generator for all operating regions by pitch angle control," *IEEE Trans. Energy Convers.*, vol. 21, no. 2, pp. 467–475, Jun. 2006.
[29] H. Geng and G. Yang, "Output power control for variable-speed variable-pitch wind generation systems," *IEEE Trans. Energy Convers.*, vol. 25, no. 2, pp. 494–503, Jun. 2010.
[30] Z. Miao, D. Alexander, and L. Fan, "Investigation of microgrids with both inverter interfaced and direct AC-connected distributed energy resources," *IEEE Trans. Power Del.*, vol. 26, no. 3, pp. 1634–1642, Jul. 2011.

ZHICHAO ZHOU received the B.Sc. degree in material engineering and the M.Sc. degree in electrical engineering from Xi'an Jiaotong University, Xi'an, China, in 2002 and 2005, respectively. He is currently pursuing the Ph.D. degree in electrical engineering with Tianjin University, Tianjin, China. His research interests include power system operation and protection, renewable energy, and distributed generation.

CHENGSHAN WANG (SM'11) received the B.Sc., M.Sc., and Ph.D. degrees from Tianjin University, Tianjin, China, in 1983, 1985, and 1991, respectively. He became a Full Professor at Tianjin University, in 1996. He was a Visiting Scientist at Cornell University, from 1994 to 1996, and as a Visiting Professor with Carneigie Mellon University, from 2001 to 2002. He is the Chief Scientist of the 973 project, "Research on the Key Issues of Distributed Generation Systems," from 2009 to 2013, that was participated by Chinese power engineering scientists from eight leading institutions. His research interests are in the area of distribution system analysis and planning, distributed generation system and microgrid, and power system security analysis. He received the Fok Ying Tung Fund, Excellent Young Teacher Fund of Education Ministry, and the winner of National Science Fund for Distinguished Young Scholars.

LEIJIAO GE (M'84) received the Ph.D. degree in electrical engineering from Tianjin University, Tianjin, China, in 2016. He is currently a Lecturer with the School of Electrical Information and Engineering, Tianjin University. His main research interests are smart grid, cloud computing, and big data.